Tohoku J. Exp. Med., 2018, **245**, 13-19

Newly-Developed Positron Emission Mammography (PEM) Device for the Detection of Small Breast Cancer

Ai Yanai,[1,5] Masatoshi Itoh,[2,4] Hisashi Hirakawa,[3] Kazuhiko Yanai,[4,5] Manabu Tashiro,[4] Ryuichi Harada,[5] Akira Yoshikawa,[6] Seiichi Yamamoto,[7] Noriaki Ohuchi[1] and Takanori Ishida[1]

[1]Department of Surgical Oncology, Tohoku University Graduate School of Medicine, Sendai, Miyagi, Japan
[2]Sendai Medical Imaging Center, Sendai, Miyagi, Japan
[3]KKR Tohoku Kosai Hospital, Sendai, Miyagi, Japan
[4]Cyclotron Radioisotope Center (CYRIC), Tohoku University, Sendai, Miyagi, Japan
[5]Department of Pharmacology, Tohoku University Graduate School of Medicine, Sendai, Miyagi, Japan
[6]Institute for Material Research, Tohoku University, Sendai, Miyagi, Japan
[7]Department of Radiological Technology, Nagoya University, Nagoya, Aichi, Japan

Positron emission mammography (PEM) has higher detection sensitivity for breast cancer compared with whole-body positron emission tomography (PET) due to higher spatial resolution. We have developed a new PEM device with high resolution over a wide field of view. This PEM device comprises novel scintillation crystals, praseodymium-doped lutetium aluminum garnet (Pr:LuAG). In the present study, the clinical use of the newly developed PEM for the detection of small breast cancer was compared with that of the conventional PET-computed tomography (PET/CT). Eighty-two patients with breast cancer less than 20 mm (UICC T1) participated in this study, including 23 patients with T1a or T1b breast cancer (less than 10 mm). Histologically-proved lesions were examined by PET/CT and PEM on the same day after injection of [^{18}F]fluoro-2-deoxy-2-fluoro-D-glucose ([^{18}F]FDG), a marker of glycolytic activity. The newly developed PEM showed better sensitivity of cancer detection compared with PET/CT especially in case of the small T1a or T1b lesions. Moreover, when the conventional PET/CT and new PEM were combined, the detection sensitivity with [^{18}F]FDG molecular imaging for T1 (N = 82) and T1a plus T1b breast cancer (N = 23) were 90% and 70%, respectively. The uptake of [^{18}F]FDG was proportional to the histological malignancy of breast cancer. Using the newly-developed PEM with [^{18}F]FDG, we are able to identify and characterize exactly the small breast tumors less than 10 mm in combination with the conventional PET/CT. These data indicate that PEM and PET/CT are synergic and complementary for the detection of small breast cancer.

Keywords: breast cancer; ^{18}F-FDG; histology; PET/CT; positron emission mammography (PEM)
Tohoku J. Exp. Med., 2018 May, **245** (1), 13-19.

Introduction

Positron-emission tomography-computed tomography (PET/CT) is effective in screening a metastatic lesion or relapse of breast cancer, but its usefulness in the diagnosis of primary lesions has not been elucidated (Fuster et al. 2008; Groheux et al. 2008, 2013; Groheux 2017). In the recent years, improved PET devices with a higher resolution have been developed. Particularly, the breast-dedicated positron emission mammography (PEM) has been reported to have a better sensitivity to a tumor that is 10 mm or smaller in size than that of PET/CT (Rosen et al. 2005; Berg et al. 2006; Eo et al. 2012; Koo et al. 2013; Kalinyak et al. 2014). Most often used crystals for detection of annihilation radiation are Lutetium Yttrium Orthosilicate (LYSO), Bismuth germanium oxide (BGO) and Gadolinium oxyorthosilicate (GSO). A research group from the Tohoku University collaboratively developed a high-resolution PEM device with two opposed detectors that utilizes new scintillation crystals praseodymium-doped lutetium aluminum garnet (Pr:LuAG) (Yanagida et al. 2010; Yoshikawa et al. 2010). Its clinical experience for the detection of small breast cancer was not reported until now. The clinical utility of this new device was compared to that of a conventional PET/CT in patients with a UICC T1 tumor that is 20 mm or smaller in size, along with the evaluation of clinical and pathological findings.

Received March 1, 2018; revised and accepted April 16, 2018. Published online May 3, 2018; doi: 10.1620/tjem.245.13.
Correspondence: Kazuhiko Yanai, M.D., Ph.D., Department of Pharmacology, Tohoku University Graduate School of Medicine, 2-1 Seiryo-machi, Aoba-ku, Sendai, Miyagi 980-8575, Japan.
e-mail: yanai@med.tohoku.ac.jp

Methods

Newly developed high-resolution PEM with an opposed detector

The PEM (PEMGRAPH; Furukawa Co., Ltd., Tsukuba, Japan), used in the present study, utilizes a pair of opposing planar detectors (23 cm × 35 cm in exterior appearance, 14 × 20 cm effective field of view) to capture annihilation photons from the breast. This device uses 10240 rectangular Pr:LuAG crystals (dimension of each crystal is 2.1 × 2.1 × 15.0 mm) and 24 units of position-sensitive photomultiplier tube (PSPMT, Hamamatsu Photonics Co., Ltd., Hamamatsu, Japan). The breast is gently compressed using a detachable and adjustable plastic plate placed between the detectors. Unlike X-ray mammography (MMG), the compression is made with a small pressure of around 50 N to hold the breast to reduce the movement due to respiration and squeeze the breast tissues into the field of view as much as possible. Although the defection of the lines of response (LOR) is unavoidable, a statistical reconstruction technique, maximum likelihood-expectation maximization (ML-EM), was employed to obtain an image at a practical level. The spatial resolution is 2.1 mm (full width at half maximum, FWHM) in the plane parallel to the detectors and the radioactive sensitivity is 9.0 cps/kBq (Yoshikawa et al. 2010; Watanabe et al. 2018).

Patients

The subjects are comprised of eighty-two patients with invasive breast cancer having a tumor that is 20 mm or smaller in size (T1), referred to the Department of Breast Surgery, KKR Tohoku Kosai Hospital between October 2015 and March 2017. Both PET/CT and PEM were performed to assess tumor extents as preoperative investigations. The PEM images of breast cancer patients were compared with the PET/CT images referring to clinic-pathological findings (Table 1). Breast cancer diagnosis was made pathologically either by fine needle aspiration under ultrasound (US) or mammotome biopsy. Around 3 weeks after the diagnosis, the patients were referred to Sendai Medical Imaging Clinic to be examined with PET/CT and the newly-developed PEM of Pr:LuAG. A written informed consent was obtained from all the patients separately at both of KKR Tohoku Kosai Hospital and Sendai Medical Imaging Clinic on this study.

Imaging with PET/CT and PEM

After at least five hours fasting, [^{18}F]fluoro-2-deoxy-2-fluoro-D-glucose ([^{18}F]FDG) (3.8 MBq/kg) was administered intravenously via the cubital vein, and a whole-body scan with PET/CT (Siemens Biograph 16; Jakoby et al. 2009) was acquired at 75 min after the FDG injection. After whole body CT, from head to pelvis, three-dimensional (3D) PET acquisition was done for 2 min per bed position. PET data were acquired using matrix of 128 × 128 pixels with a slice thickness of 3 mm. CT-based attenuation correction of the emission images was used. PET images were reconstructed by iterative ordered subset expectation maximization (OSEM; four iterations and eight subsets) using 5 mm Gaussian kernel. In this setting the PET spatial resolution was approximately 7 mm FWHM. After PET/CT scan the PEM scan was consecutively performed at around 100 min after the FDG injection at 3-5 min duration in the mediolateral (ML) direction with 15 cm detector separation. Imaging with 20 cm detector separation is added to have wider field of view of the chest wall (tangential chest wall scan) in case of thin breast or when the tumor is located in the margin of the breast. The PET/CT and PEM images were independently evaluated by two radiologists/nuclear medicine physicians. Visibility of breast cancer was defined as positive when an isolated hot spot is visually identified exactly at the location pointed out by ultrasound using both the quadrant and clock face notation and the distance from the nipple.

The present PET/CT and PEM study was conducted with the approval of both of the ethics committees of KKR Tohoku Kosai Hospital and Sendai Medical Imaging Clinic. This study was also approved by the Ethics Committee of Tohoku University Graduate School of Medicine (No.2017-1-413) and performed in accordance with the Declaration of Helsinki.

Statistical analysis

The use of standardized uptake value (SUV) is now common place in clinical FDG-PET/CT oncology imaging. For the PEM studies, the semi-quantitative the maximum PEM-uptake value (PUV) was calculated using the following formula: tissue concentration (mCi/g) × body weight (g) / injected FDG dose (mCi). This formula is the same as SUV, but tissue attenuation of photons by breast tissue is not corrected in the PEM examination. The relationship between the tumor/background (T/B) ratio of PET/CT and PEM was examined using Pearson's correlation test. The T/B ratios of PET/CT and PEM were analyzed by both of paired t-test and Wilcoxon single-ranks test. The PUVs among the pathological findings of luminal type, HER2 type and Triple Negative Group (TNG) type were examined by Kruskal-Wallis test for multiple non-parametric comparisons. The difference in PUVs between the degree of pathological malignancy was examined using a non-parametric Mann-Whitney's U test. The level of statistical significance was set at $p < 0.05$. All statistical analyses were performed on BellCurve for Excel (BellCurve BU, Tokyo, Japan).

Results

Utility of the newly developed PEM

Table 1 shows the characteristics of the 82 patients with invasive breast cancer whose tumor is 20 mm or smaller in size (T1), summarizing tumor detectability with either PET/CT or PEM or both combined performed before surgery in KKR Tohoku Kosai Hospital between October 2015 and March 2017. Fig. 1 depicts a representative case of an invasive ductal carcinoma (13 × 9 × 8 mm in size) that was detected via medical screening. The MMG pointed out a focal asymmetric density (FAD) of category 3, in the upper outer C quadrant with a high FDG uptake in both PET/CT and PEM images. The sensitivity and resolving power of the newly developed PEM are 2-3 times higher than those of conventional PET/CT (Siemens Biograph). Other examples that show the superiority of PEM over PET/CT are presented in Fig. 2. In Fig. 2A, a small breast tumor of 4 mm in size with ultrasound was clearly depicted with PEM which were not detectable with PET/CT. In Fig. 2B, small hot nodules more than three in number, were resolved with PEM while only a single tumor was visible with the PET/CT.

Comparison of the performance of PET/CT and PEM to detect breast cancer

Fig. 3 shows the relationship between PET/CT and

Table 1. Patient characteristics.

Age (N = 82)	57 ± 10.9 (mean ± SD)
Subtype	
Luminal	67 (82 %)
HER2	5 (6 %)
TNG	10 (12 %)
T	
1a	5 (6 %)
1b	18 (22 %)
1c	59 (72 %)
N	
N0	62 (76 %)
N1	19 (23 %)
N2	1 (1 %)
N3	0 (0 %)
NG	
NG1	45 (55 %)
NG2	6 (7 %)
NG3	22 (26 %)
nd	9 (11 %)
HG	
HG1	33 (40 %)
HG2	22 (27 %)
HG3	18 (22 %)
nd	9 (11 %)
Ki-67	22.7 ± 15.8 (mean ± SD)
< 20	45 (55 %)
≧20	24 (29 %)
nd	13 (16 %)

nd, not determined.

PEM as assessed by the T/B ratio at the tumor site. The correlation coefficient (R^2) was 0.64 in all patients with a T1 lesion and 0.87 in patients with T1a/1b lesion (less than 10 mm), both showing a favorable correlation (Pearson's correlation coefficient test; $P < 0.0001$). In all patients with a T1 lesion, the mean T/B ratio was 3.8 ± 3.6 in PET/CT and 3.3 ± 2.1 in PEM, showing no statistical difference (paired t-test and Wilcoxon single-ranks test: $p > 0.1$). In patients with T1a/1b lesions, the mean T/B ratio was 1.6 ± 0.9 in PET/CT and 2.3 ± 2.0 in PEM, showing that PEM was significantly higher than PET (paired t-test and Wilcoxon single-ranks test: $p < 0.01$). This result reflects the fact that PEM has better sensitivity of cancer detection than PET/CT in the small T1a/1b lesions because of its higher resolution.

Table 2 shows the detection rate of PEM and PET/CT in all T1 (82 cases). In all patients with a T1 lesion, the detection sensitivities of PET/CT, PEM, and PET/CT and PEM were 82%, 85%, and 90%, respectively, showing no statistical difference. However, the diagnostic sensitivity slightly increased when used PET and PEM together. In 23 patients with a T1a/1b lesion that is smaller than T1c (10 mm < tumor size ≤ 20 mm), the detection sensitivities of PET/CT, PEM, and PET/CT and PEM were 48%, 65%, and 70%, respectively, showing a similar result (Table 3). Most of the cases in which a lesion was detectable with PEM but was undetectable with PET/CT were categorized in T1a/1b cases. All cases in which a lesion was not detectable with PEM are those with regions of upper inner quadrant A.

Pathological findings and PUV

The pathological findings and PUV obtained before surgery were compared. As shown in Fig. 4, when the PUV was compared based on subtype, the average PUV of the luminal type A+B, HER2 type, and TNG type were 3.3 ± 1.8, 3.9 ± 1.0, and 4.7 ± 1.4 (mean ± SD), indicating that

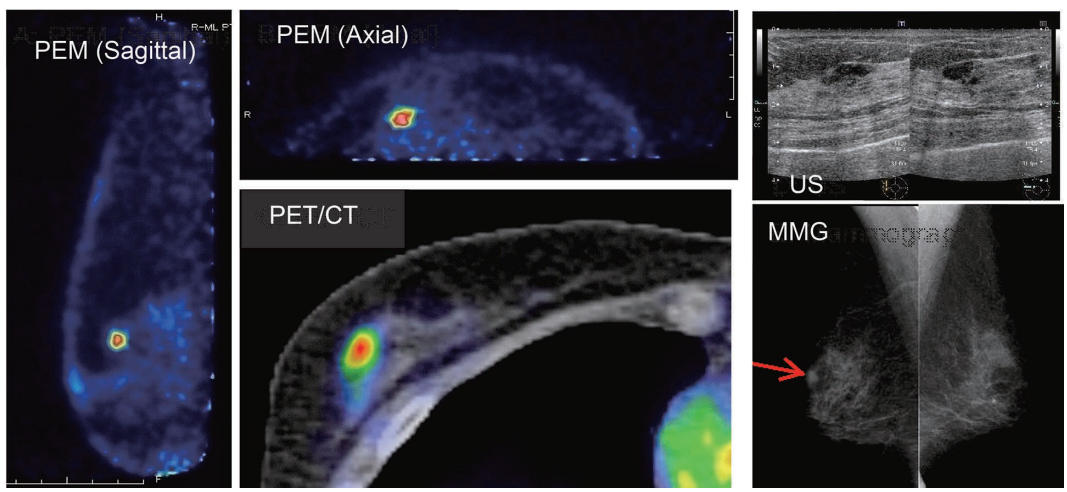

Fig. 1. Comparison of the newly-developed PEM, PET/CT, US, and MMG in a typical case of an invasive ductal carcinoma (13 × 9 × 8 mm in size).
The MMG and US delineated a focal asymmetric density. The PET/CT and PEM images showed round spots and irregular spots of high FDG uptake of breast cancer, respectively.

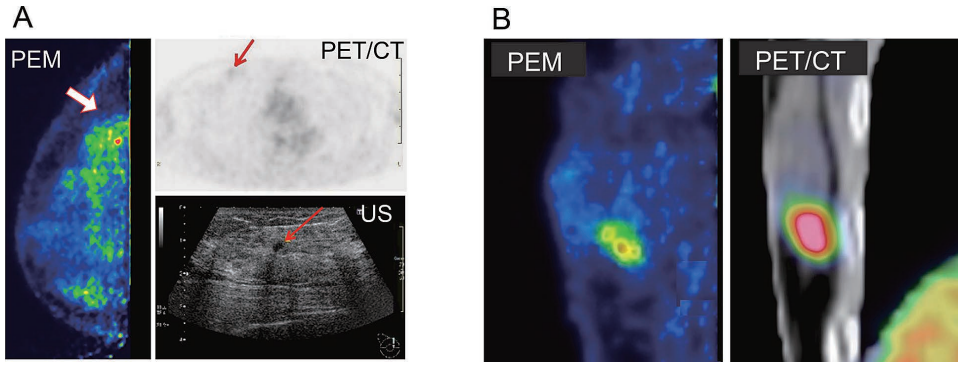

Fig. 2. Image that shows the superiority of the newly-developed PEM.
A: A case with micro-invasive carcinoma (4 mm in size). PEM is superior to PET/CT for the detection of small breast cancer less than 10 mm. B: Image that shows the higher resolving power of PEM than PET/CT.

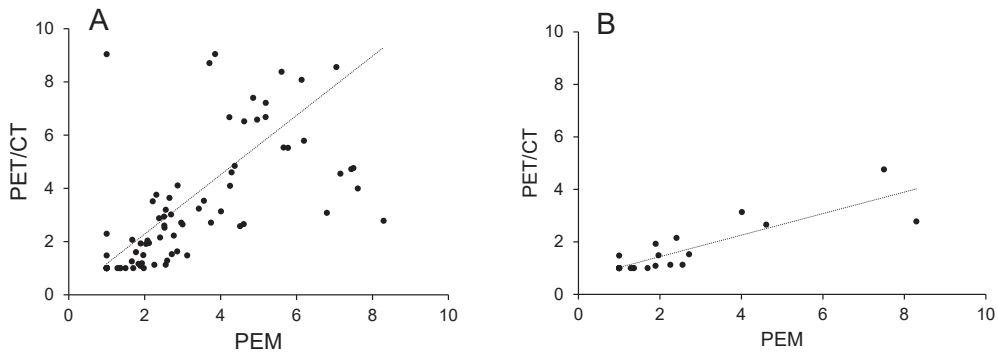

Fig. 3. Relationship between the newly-developed PEM and PET/CT in the tumor/background ratio (T/B).
A: T/B in all patients with T1 lesions (N = 82). B: T/B in patients with a T1a/1b lesions (N = 23). Note that the slope of T1a/1b cases are shallow, indicating the sensitivity of PEM is higher than that in PET/CT in small breast cancer.

Table 2. Sensitivity of all T1 cases.

		PEM	
		Not Detected	Detected
PET/CT	Not Detected	8	7
	Detected	4	63

Sensitivity: PET 82%; PEM 85%; PET+PEM 90%.

Table 3. Sensitivity of T1a and T1b cases.

		PEM	
		Not Detected	Detected
PET/CT	Not Detected	7	5
	Detected	1	10

Sensitivity: PET 48%; PEM 65%; PET+PEM 70%.

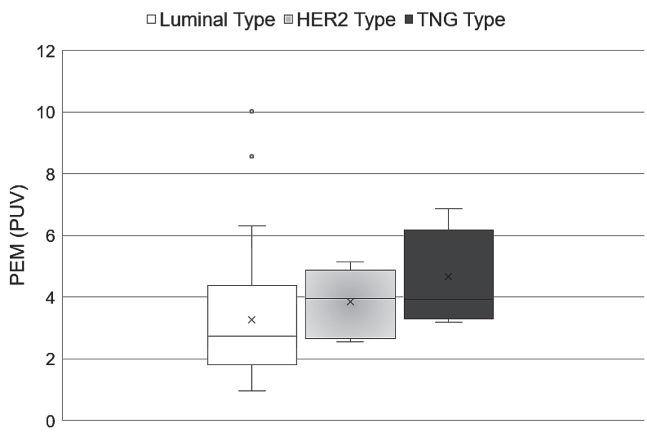

Fig. 4. Differences between the pathological findings.
The PUVs obtained by the PEM were compared among Luminal A and B (N = 67), HER2 (N = 5), and Triple Negative Group (TNG: N = 10).

the PUV increases in the order of Luminal A+B < HER 2 type < TNG. Moreover, a slight difference was observed among these 3 subtypes (Kruskal-Wallis test: P = 0.035).

Fig. 5 shows the relationship between the degree of pathological malignancy and the PUV. The PUV was 3.0 ± 1.7 (mean ± SD) in Nuclear grade (NG) 1-2 and 4.4 ± 1.8 in NG3, showing a significant difference (Fig. 5A; Mann-Whitney's U test P < 0.01). When a cutoff value of 20 was used for Ki-67, the PUV was 3.1 ± 1.8 (mean ± SD) in Ki-67 of < 20 and 4.1 ± 1.5 in Ki-67 of ≥ 20, showing a significant difference (Fig. 5B; Mann-Whitney's U test P < 0.01). In other words, these results indicate that the PUV

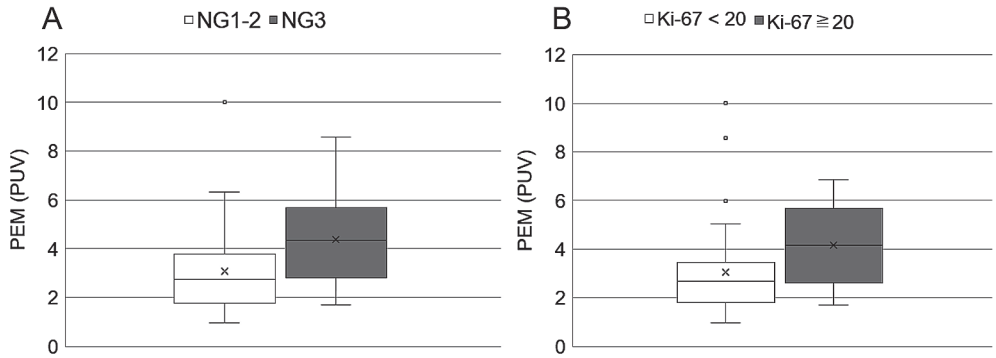

Fig. 5. Difference between the degree of histological malignancy and PUV obtained by the PEM.
A: Nuclear grade (NG) scores. NG1-2 (N = 51) and NG3 (N = 22). B: Ki-67. Ki-67 < 20 (N = 45) and Ki-67 ≥ 20 (N = 24).

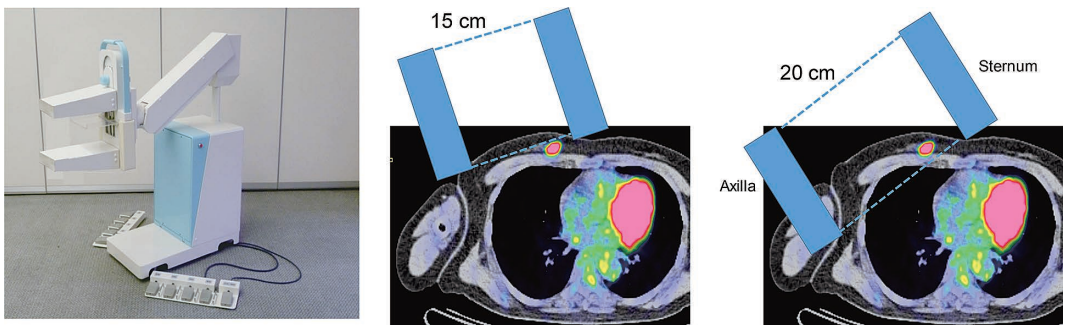

Fig. 6. Appearance of newly developed PEM and improvement of the area of visualization.
The appearance of the newly-developed PEM device is shown. The distance between the detectors can be adjusted from 5 cm to 25 cm. The area of visualization can be increased by some adjustments to include the tumors residing in the region proximal to the chest wall or in the thin breast.

increases with the degree of malignancy.

Discussion

A research group from the Tohoku University and Furukawa Co., Ltd. collaboratively developed a high-resolution PEM device with opposed detectors that utilizes new scintillation crystals of Pr:LuAG, which has not been used before for PET or PEM. Pr:LuAG has almost twice as shorter scintillation decay time than that of LYSO (Yoshikawa et al. 2010). Pr:LuAG is expected to produce PEM images with a better signal-to-noise ratio in high count rate study as compared to the commonly used LYSO. Yoshikawa et al. (2010) evaluated the clinical utility of PEMGRAPH for the diagnosis of breast cancer lesions that are 20 mm or smaller in size. Characteristically, the newly developed PEM has better radiation sensitivity than conventional PET/CT, which may reduce the amount of FDG injection. In addition, the newly-developed PEM has a high resolution similar to other commercially-available PEM scanners (Caldarella et al. 2014). Another benefit of PEM is that no extra radiation is required for the study when PEM is carried out sequentially after PET/CT examination.

In the present study, the T/B ratio of a tumor that is 10 mm or smaller in size (T1a/1b cases) was significantly higher in PEM than in PET/CT. Most of the cases in which a lesion was detectable with PEM but was undetectable with PET/CT were categorized in T1a/1b cases, suggesting the good utility of PEM in the detection of a tumor that is 10 mm or less. Concerning the location of the tumor in the breast, tumors in the upper inner quadrant, quadrant A, were most difficult to be identified with PEM followed by the lower inner quadrant, quadrant B. The breast areas close to the sternum must be blind areas for PEM. Therefore, we employed the chest-wall scan that is a tangential imaging of breast tissue opening the detector distance up to 20 cm. The chest-wall scan may be a solution to reduce blind breast areas although the spatial resolution is lost in some extent along the direction perpendicular to the detectors as shown in Fig. 6. The specificity of PEM was reported to be better than that of MRI (Caldarella et al. 2014). We need further studies to mention on this topic. However, based on the present study of PEM, we need to gather the data of the patients who underwent both PET/CT and PEM before preoperative histological biopsy because the detectability of the small tumors with further PET/CT or PEM decreases after biopsy.

A significantly higher PUV was observed in cases with NG-3 and Ki-67 ≥ 20, suggesting that a good correlation between glucose metabolism and the nuclear grade score and Ki-67. These results were supported by the comparison of the subtypes wherein the highly malignant triple negative type often had a high PUV, while the less malignant luminal

types had a low PUV. Thus, the estimation of the degree of malignancy may be made with PEM imaging especially in the early stage of breast cancer taking advantage of high resolution (Basu et al. 2008; Groheux et al. 2011; Bitencourt et al. 2017). In addition, the use of other probes may be useful for the future applications PET/CT and PEM. It is reported that ^{18}F-fluoroestradiol (estrogen receptor binding) and ^{68}Ga-ABY025 (HER2-binding affibody) can predict the therapy responses (Peterson et al. 2014; Sörensen et al. 2016; Kurland et al. 2017).

Because the detection rate of breast cancer with whole-body PET/CT screening health check was reported to be 0.18%-0.23% of healthy population, the use of PET/CT is not recommended as a screening method for breast cancer. With an improved resolution of PEM, some research showed that the detection rate of PEM was 2.3%, which is better than that of PET/CT (Yamamoto et al. 2015, 2016). Other research suggested that the sensitivity of PEM is significantly better than that of PET in tumors that are 20 mm or smaller in size (Eo et al. 2012).

Using the newly-developed PEM device that utilizes scintillation crystals of Pr:LuAG, Watanabe et al. (2018) demonstrated that resected specimen-PEM examination delineated tumor extension in breast-conserving surgery. The results of our study have following limitations. Because of the small sample size, some statistical analyses could have been affected. On the other hand, the present study has demonstrated that the sensitivity is better with PEM for tumors that are 10 mm or smaller in size. However, in all tumors, no significant difference was observed in the tumor detection sensitivity of PEM and PET/CT in UICC T1 cases. One of drawbacks of the present study is that we evaluated tumor FDG uptake by one or zero, that is detected or not detected. Further studies are needed taking account of count recovery of FDG uptake in tumors that is crucially affected by the spatial resolution.

The detection rate and accuracy can be improved by using both PET/CT and PEM combined over whole-body PET/CT alone. PET/CT is useful to assess tumor spreads in the whole body, while PEM can be used to assess tumor extent and spreads within the breast in a synergic and complimentary manner. Considering that the resolution of PEM can be further improved using smaller scintillation crystals and larger numbers of electronics, new PEM techniques may reach metabolic and pathological imaging of tumors with less than 10 mm. Further studies correlating PEM imaging, pathological and molecular features could help us to better understanding of breast cancers and their tissue heterogeneity that leads to proper personalized management of breast cancer.

Acknowledgments

This work was partially supported by a Grant-in-Aid for challenging Exploratory Research (16K15314), Japan Society of Promotion for the Promotion of Science (JSPS). We appreciate Professor Hiroshi Watabe (CYRIC) and Mr. Shoichi Watanuki for discussing the manuscript. The authors also thank Drs. Rie Sugai and Katsuhiko Shibuya for supporting PET/CT and PEM imaging.

Conflict of Interest

The PEM used in the present study was developed through a collaborative research by Furukawa Scintitech Corporation, Sendai Medical Imaging Center, and Cyclotron and Radioisotope Center, Tohoku University. The Pr:LuAG scintillation crystals were patented by Tohoku University. The authors declare no conflict of interest.

References

Basu, S., Chen, W., Tchou, J., Mavi, A., Cermik, T., Czerniecki, B., Schnall, M. & Alavi, A. (2008) Comparison of triple-negative and estrogen receptor-positive/progesterone receptor-positive/HER2-negative breast carcinoma using quantitative fluorine-18 fluorodeoxyglucose/positron emission tomography imaging parameters: a potentially useful method for disease characterization. *Cancer*, **112**, 995-1000.

Berg, W.A., Weinberg, I.N., Narayanan, D., Lobrano, M.E., Ross, E., Amodei, L., Tafra, L., Adler, L.P., Uddo, J., Stein, W. 3rd & Levine, E.A.; Positron Emission Mammography Working Group (2006) High-resolution fluorodeoxyglucose positron emission tomography with compression ("positron emission mammography") is highly accurate in depicting primary breast cancer. *Breast J*., **12**, 309-323.

Bitencourt, A.G., Lima, E.N., Macedo, B.R., Conrado, J.L., Marques, E.F. & Chojniak, R. (2017) Can positron emission mammography help to identify clinically significant breast cancer in women with suspicious calcifications on mammography? *Eur*. *Radiol.*, **27**, 1893-1900.

Caldarella, C., Treglia, G. & Giordano, A. (2014) Diagnostic performance of dedicated positron emission mammography using fluorine-18-fluorodeoxyglucose in women with suspicious breast lesions: a meta-analysis. *Clin*. *Breast Cancer*, **14**, 241-248.

Eo, J.S., Chun, I.K., Paeng, J.C., Kang, K.W., Lee, S.M., Han, W., Noh, D.Y., Chung, J.K. & Lee, D.S. (2012) Imaging sensitivity of dedicated positron emission mammography in relation to tumor size. *Breast*, **21**, 66-67.

Fuster, D., Duch, J., Paredes, P., Velasco, M., Muñoz, M., Santamaría, G., Fontanillas, M. & Pons, F. (2008) Preoperative staging of large primary breast cancer with [^{18}F]fluorodeoxyglucose positron emission tomography/computed tomography compared with conventional imaging procedures. *J. Clin. Oncol.*, **26**, 4746-4751.

Groheux, D. (2017) FDG-PET/CT for systemic staging of patients with newly diagnosed breast cancer. *Eur. J. Nucl. Med. Mol. Imaging*, **44**, 1417-1419.

Groheux, D., Espié, M., Giacchetti, S. & Hindié E. (2013) Performance of FDG PET/CT in the clinical management of breast cancer. *Radiology*, **266**, 388-405.

Groheux, D., Giacchetti, S., Moretti, J.L., Porcher, R., Espié, M., Lehmann-Che, J., de Roquancourt, A., Hamy, A.S., Cuvier, C., Vercellino, L. & Hindié, E. (2011) Correlation of high ^{18}F-FDG uptake to clinical, pathological and biological prognostic factors in breast cancer. *Eur. J. Nucl. Med. Mol. Imaging*, **38**, 426-435.

Groheux, D., Moretti, J.L., Baillet, G., Espie, M., Giacchetti, S., Hindie, E., Hennequin, C., Vilcoq, J.R., Cuvier, C., Toubert, M.E., Filmont, J.E., Sarandi, F. & Misset, J.L. (2008) Effect of ^{18}F-FDG PET/CT imaging in patients with clinical Stage II and III breast cancer. *Int. J. Radiat. Oncol. Biol. Phys.*, **71**, 695-704.

Jakoby, B.W., Bercier, Y., Watson, C.C., Bendriem, B., Townsend, D.W. (2009) Performance characteristics of a new LSO PET/

CT scanner with extended axial field-of-view and PSF reconstruction. *IEEE Trans. Nucl. Sci.*, **56**, 633-639.

Kalinyak, J.E., Berg, W.A., Schilling, K., Madsen, K.S., Narayanan, D. & Tartar, M. (2014) Breast cancer detection using high-resolution breast PET compared to whole-body PET or PET/CT. *Eur. J. Nucl. Med. Mol. Imaging*, **41**, 260-275.

Koo, H.R., Moon, W.K., Chun, I.K., Eo, J.S., Jeyanth, J.X., Chang, J.M., Cho, N. & Kang, K.W. (2013) Background ^{18}F-FDG uptake in positron emission mammography (PEM): correlation with mammographic density and background parenchymal enhancement in breast MRI. *Eur. J. Radiol.*, **82**, 1738-1742.

Kurland, B.F., Peterson, L.M., Lee, J.H., Schubert, E.K., Currin, E.R., Link, J.M., Krohn, K.A., Mankoff, D.A. & Linden, H.M. (2017) Estrogen receptor binding (^{18}F-FES PET) and glycolytic activity (^{18}F-FDG PET) predict progression-free survival on endocrine therapy in patients with ER+ breast cancer. *Clin. Cancer Res.*, **23**, 407-415.

Peterson, L.M., Kurland, B.F., Schubert, E.K., Link, J.M., Gadi, V.K., Specht, J.M., Eary, J.F., Porter, P., Shankar, L.K., Mankoff, D.A. & Linden, H.M. (2014) A phase 2 study of 16α-[^{18}F]-fluoro-17β-estradiol positron emission tomography (FES-PET) as a marker of hormone sensitivity in metastatic breast cancer (MBC). *Mol. Imaging Biol.*, **16**, 431-440.

Rosen, E.L., Turkington, T.G., Soo, M.S., Baker, J.A. & Coleman, R.E. (2005) Detection of primary breast carcinoma with a dedicated, large-field-of-view FDG PET mammography device: initial experience. *Radiology*, **23**, 527-534.

Sörensen, J., Velikyan, I., Sandberg, D., Wennborg, A., Feldwisch, J., Tolmachev, V., Orlova, A., Sandström, M., Lubberink, M., Olofsson, H., Carlsson, J. & Lindman, H. (2016) Measuring HER2-receptor expression in metastatic breast cancer using [^{68}Ga]ABY-025 affibody PET/CT. *Theranostics*, **6**, 262-271.

Watanabe, G., Itoh, M., Duan, X., Watabe, H., Mori, N., Tada, H., Suzuki, A., Miyashita, M., Ohuchi, N. & Ishida, T. (2018) ^{18}F-Fluorodeoxyglucose specimen-positron emission mammography delineates tumor extension in breast-conserving surgery: Preliminary results. *Eur. Radiol.*, **28**, 1929-1937.

Yamamoto, Y., Ozawa, Y., Kubouchi, K., Nakamura, S., Nakajima, Y. & Inoue, T. (2015) Comparative analysis of imaging sensitivity of positron emission mammography and whole-body PET in relation to tumor size. *Clin. Nucl. Med.*, **40**, 21-25.

Yamamoto, Y., Tasaki, Y., Kuwada, Y., Ozawa, Y. & Inoue, T. (2016) A preliminary report of breast cancer screening by positron emission mammography. *Ann. Nucl. Med.*, **30**, 130-137.

Yanagida, T., Yoshikawa, A., Yokota, Y., Kamada, K., Usuki, Y., Yamamoto, S., Miyake, M., Baba, M., Kumagai, K., Sasaki, K., Ito, M., Abe, N., Fujimoto, Y., Maeo, S., Furuya, Y., et al. (2010) Development of Pr:LuAG Scintillator Array and Assembly for Positron Emission Mammography. *IEEE Trans. Nucl. Sci.*, **57**, 1492-1495.

Yoshikawa, A., Yanagida, T., Kamada, K., Yokota, Y., Pejchal, J., Yamaji, A., Usuki, Y., Yamamoto, S., Miyake, M., Kumagai, K., Sasaki, K., dos Santos, T.R., Baba, M., Ito, M., Takeda, M., et al. (2010) Positron emission mammography using Pr:LuAG scintillator: fusion of optical material study and systems engineering. *Optical Materials*, **32**, 1294-1297.